Association Forms of NO in Sodium Ion-Exchanged A-Type Zeolite: Temperature-Dependent Q-Band EPR Spectra

Hidenori Yahiro,[†] Anders Lund,*[,‡] Roland Aasa,[§] Nikolas P. Benetis,[||] and Masaru Shiotani[||]

Chemical Physics Laboratory, IFM Linköping University, S-581 83 Linköping, Sweden, Department of Applied Chemistry, Faculty of Engineering, Ehime University, Matsuyama 790-8577, Japan, Department of Molecular Biotechnology, Chalmers University of Technology, Lundberg Laboratory, P. O. Box 462, SE-405 30 Göteborg, Sweden, and Department of Applied Chemistry, Faculty of Engineering, Hiroshima University, Higashi-Hiroshima 739-8527, Japan

Received: March 14, 2000; In Final Form: June 8, 2000

Nitrogen monoxide (NO) introduced into sodium ion-exchanged A-type (Na-A) zeolite was studied by temperature- and NO pressure-dependent EPR measurements at Q-band in the temperature range between 5 and 140 K. The experimental spectra were successfully utilized to determine accurate values of the $\boldsymbol{g}$ and $\boldsymbol{A}(^{14}N)$ tensors of NO monoradical and the $\boldsymbol{g}$ tensors and zero field splitting (ZFS) parameters, D and E, of the NO−NO biradical. Two different EPR spectra corresponding to low and high temperature forms of the NO monoradical were observed when the NO pressure was low ($P_{NO} \leq 3.1$ kPa). Based on the $\boldsymbol{g}$ and $\boldsymbol{A}$ tensors, the former was attributed to a rigid form and the latter to a rotational form of the monoradical. For higher NO pressure, the biradical became dominant. The structure of the biradical was discussed in terms of the $\boldsymbol{D}$ and $\boldsymbol{g}$ tensors combined with the spectral line shape simulation method.

Introduction

Understanding of the adsorbed state of NO in cation-exchanged zeolites is extremely important from a catalysis point of view, because it has been recognized that the zeolites exhibit high catalytic performances for NO decomposition and NO selective catalytic reduction.[1] Lunsford[2] has first reported EPR spectra of NO molecules adsorbed on sodium ion exchanged Y-type zeolite. After this report, a number of EPR studies of NO adsorbed on zeolites were performed, e.g., for Na-A, Ca-A, Na-X, and H-mordenite,[3] Na-, Ba- and Zn−Y zeolites,[4] and H- and Na−ZSM-5,[5] indicating formation of NO monoradical in the zeolites. Kasai and Bishop[6] analyzed the spectra of adsorbed NO on Y-type zeolite with different cations, and they concluded that NO molecules were attached to the cations in a bent configuration.

Kasai and Gaura[7] have reported the formation of a biradical, NO−NO radical pair, in Na-A zeolites. They observed X-band EPR signal due to the forbidden transition, $|\Delta M_S| = 2$, at ca. 1700 G ($g \cong 4$), when the corresponding allowed transitions, $|\Delta M_S| = 1$, were observed for the same sample at ca. 3400 G ($g \cong 2$). This verified the presence of a triplet biradical species. However, the signals of the NO monoradical and the NO biradical were superimposed in the X-band EPR at 77 K in a way that obscured the spectrum of the individual species. In the present work, to obtain spectra with better resolution, Q-band EPR measurements in the temperature range 5−140 K were carried out for NO introduced in sodium ion-exchanged A-type (Na-A) zeolites. The EPR parameters ($\boldsymbol{g}$, $\boldsymbol{A}(^{14}N)$, D, and E) obtained by simulations of the Q-band spectra were considerably improved compared to those obtained by using merely X-band simulations.

Experimental Section

Na-A zeolites used in the present study were supplied by Tosoh Co. Approximately 0.05 g of Na-A zeolite was placed in a 4 mm- or a 2 mm-quartz tube for X- or Q-band EPR measurements, respectively. The sample was maintained at 473 K for 1 h in air, followed by heating to 673 K in a vacuum. After keeping the temperature at 673 K for 1 h, the sample was exposed to oxygen (5 kPa) to oxidize some organic impurities on the zeolite, evacuated for 30 min, and then cooled to room temperature. The sample was exposed to NO (0.1−13.2 kPa) at room temperature at least for 24 h. Powder X-ray diffractometry was performed to examine the structure of the Na-A zeolite before and after heat treatment at 673 K, and it was ascertained that no change occurred in the structure of the zeolite even after the heat treatment.

X-band EPR spectra were recorded with a Bruker ER-200 D spectrometer. The microwave power was adjusted to avoid saturation. The magnetic field was calibrated with a Bruker ER 035 NMR gaussmeter. The temperature of measurement from 4 to 110 K was controlled using an Oxford EPR-9 He flow cryostat. Q-band spectra at 34 GHz were recorded with a Bruker ESP 380 E spectrometer using an ER 050 QG bridge and an ER 5103 QT cavity. Low temperatures were obtained by a Bruker Flexline 4118 CF helium cryostat. The spectral line-shape simulations of the allowed transitions were performed using the Bruker program, Simfonia.

Results

Kasai and Gaura[7] have reported the X-band spectra of NO adsorbed on Na-A zeolites recorded at 77 K. They found that the spectra observed at $g \cong 2$ could be interpreted by assuming

* Corresponding author. E-mail, alund@ifm.liu.se. Fax +46-13-137568.
[†] Ehime University.
[‡] IFM Linköping University.
[§] Chalmers University of Technology.
[||] Hiroshima University.

10.1021/jp0009709 CCC: $19.00
Published on Web 08/03/2000

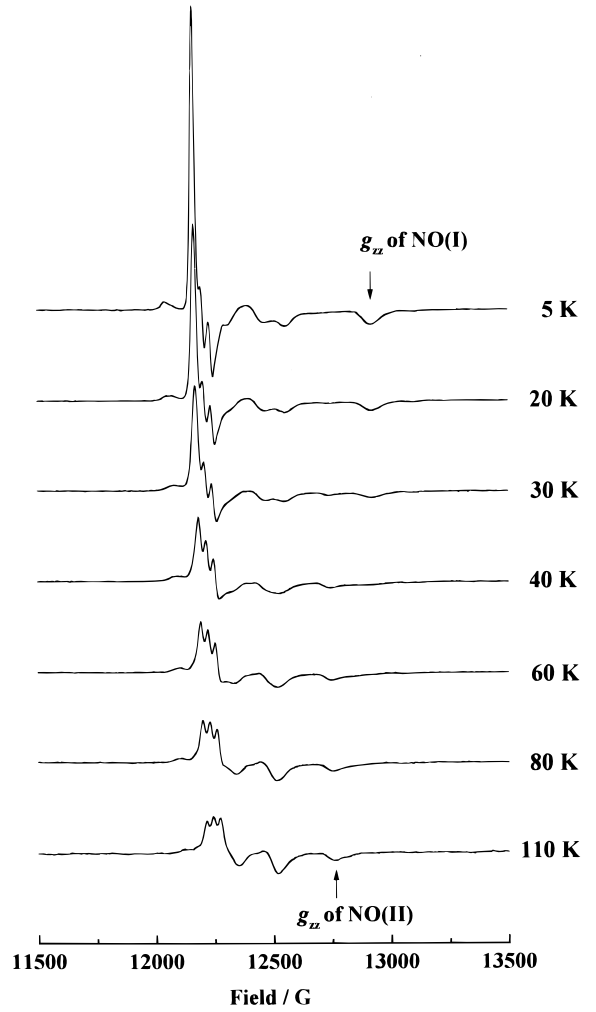

Figure 1. Q-band EPR spectra of NO (3.1 kPa) introduced in Na-A zeolite as a function of temperature in the temperature range of 5 to 110 K. The microwave frequency was 34.095 GHz.

the superposition of two sets of spectra. One was assigned to a single NO molecule adsorbed on a Na cation (NO monoradical[2−5]) and the other was attributed to a NO−NO dimeric triplet species (NO biradical). The monoradical spectrum was characterized by three different resolved *g* tensor components and a resolved *y*-component of the ^{14}N hyperfine coupling. The biradical spectrum was characterized by both *g*- and zero-field splitting tensor anisotropies, but the ^{14}N hyperfine splitting was not resolved. Similar X-band spectra were observed also in the present work, including new details about the temperature dependence of the EPR spectra; however, the superposition of the powder-spectrum patterns of monoradical and biradical species made it difficult to determine the precise EPR parameters of both radicals. Therefore, Q-band EPR measurements were carried out in order to obtain spectra with better resolution of the $\boldsymbol{g}$ tensors.

In Figures 1 and 2, the temperature dependence of Q-band EPR spectra for NO adsorbed on Na-A zeolites is depicted for 3.1 and 13.2 kPa of NO pressure, respectively. The pressure dependence of X-band EPR spectra reported by us[8] and by Kasai and Gaura,[9] suggests that the NO monoradical dominates when the pressure is low ($P_{NO} \leq 0.1$ kPa), while the NO biradical becomes dominant at higher NO pressure ($P_{NO} \geq 10$ kPa). Therefore, the assignment of NO monoradical was performed in samples with relatively low NO pressure ($P_{NO} = 3.1$ kPa).

The spectrum recorded at the lowest temperature in this work at 5 K, shown in Figure 1, was first simulated only for the bands

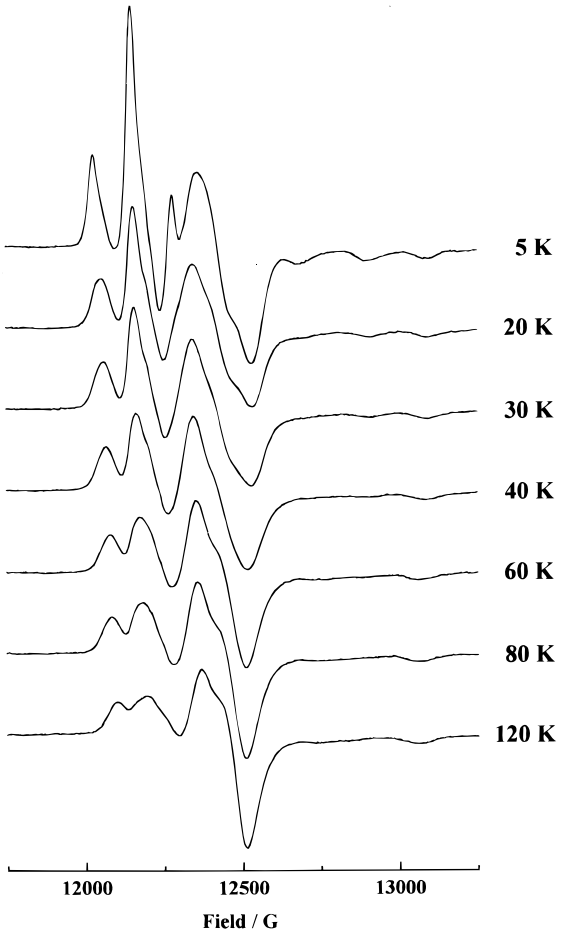

Figure 2. Q-band EPR spectra of NO (13.2 kPa) introduced in Na-A zeolite as a function of temperature in the temperature range of 5 to 120 K. The microwave frequency was 34.095 GHz.

of NO monoradical. The experimental and simulated spectra are shown in Figure 3(A). The spectral peaks corresponding to the NO monoradical were successfully simulated using the resolved *g*-tensor components and the *y*-component of the ^{14}N hyperfine tensor $\boldsymbol{A}(^{14}\mathrm{N})$. The resulting best-fit EPR parameters are $g_{xx} = 2.0019$, $g_{yy} = 1.9961$, $g_{zz} = 1.8856$ and $A_{xx}(^{14}\mathrm{N}) = A_{zz}(^{14}\mathrm{N}) = 0$ G, $A_{yy}(^{14}\mathrm{N}) = 33$ G. Using the $\boldsymbol{g}$ and $\boldsymbol{A}(^{14}\mathrm{N})$ principal values determined from the Q-band spectral fitting, the X-band spectrum was simulated as shown in Figure 3(B). Clearly, there is excellent agreement between the experimental and the calculated spectra. This NO monoradical is denoted by NO(I) or type I of NO from now on.

The band at ca. 12 920 G, which was attributed to the g_{zz} component of NO(I) observed at 5 K, became weaker and broader with increasing temperature and invisible above 40 K as seen in Figure 1; the line widths of the first derivative spectra were, for example, ca. 60 G at 5K and ca. 90 G at 30 K. Simultaneously, the signal intensity at the g_{xx} and g_{yy} components of NO(I) decreased with increasing temperature up to 40 K, while a new band at ca. 12 750 G became visible at 20 K and grew up gradually with increasing temperature to 110 K. The NO radical corresponding to this new band is denoted by NO(II) or type II of NO. The spectral change between NO(I) and NO(II) was reversible in the temperature range between 5 and 100 K. Furthermore, the total radical concentration remained unchanged in the temperature range.

To determine the EPR parameters of NO(II), the spectrum recorded at 110 K, which is expected to be completely unaffected by the signal of NO(I) monoradical, was simulated

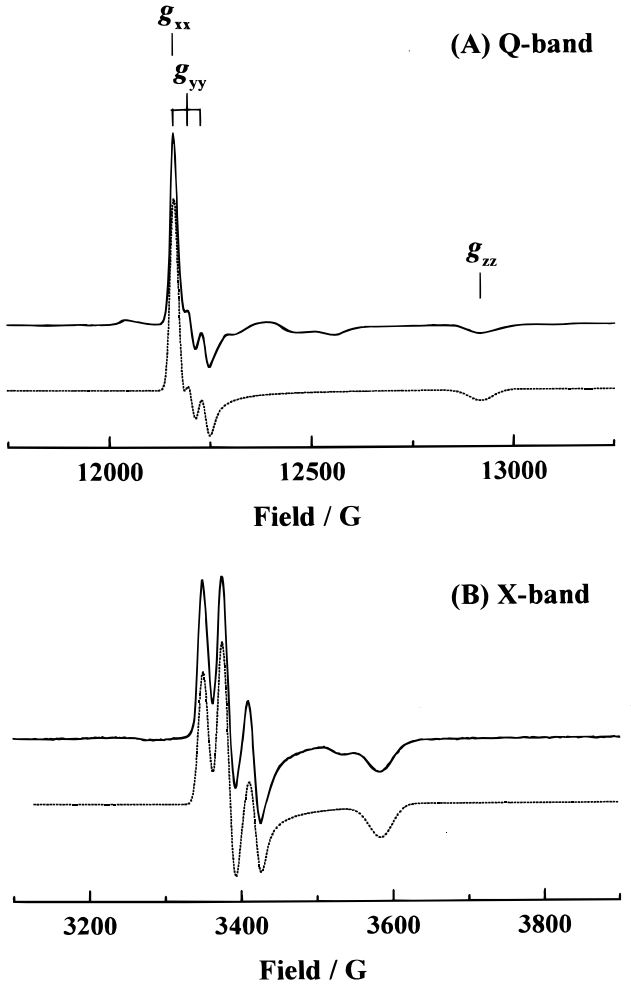

Figure 3. (A) Experimental (solid line) and simulated (dotted line) Q-band EPR spectra of NO (3.1 kPa) introduced in Na-A zeolite at 5 K. The simulation of the NO(I) spectrum was performed using Lorentzian line shape with anisotropic line width of 19, 21, and 50 G for the *x*, *y*, and *z* components, respectively. The other parameters used are given in Table 1. (B) X-band spectrum (dotted line) calculated using the parameters determined from the Q-band simulation compared with the experimental one (solid line) that was recorded for 0.1 kPa NO introduced in Na-A zeolite at 4.2 K.

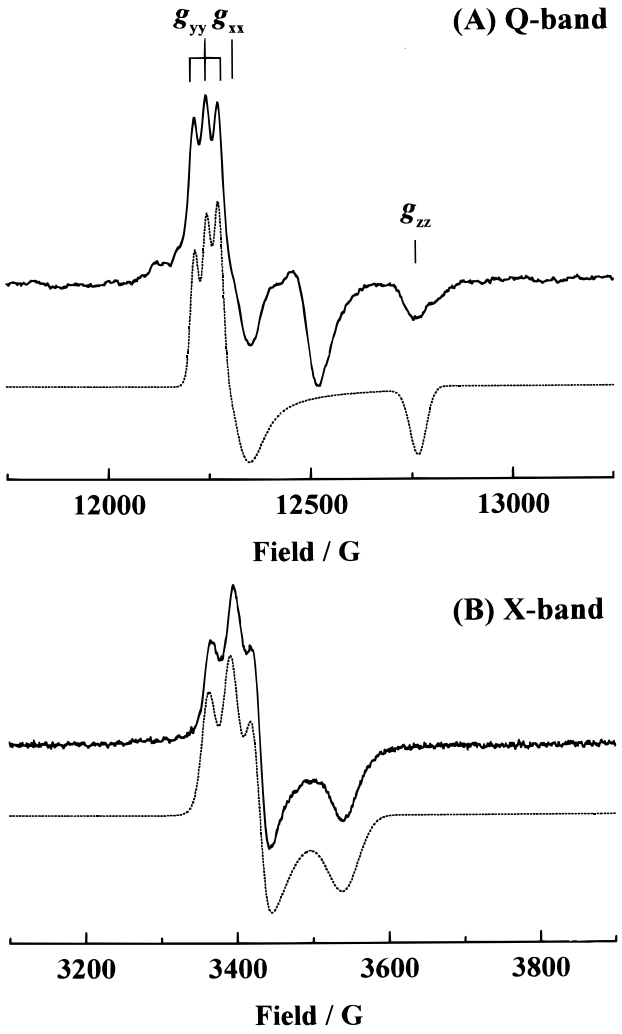

Figure 4. (A) Experimental (solid line) and simulated (dotted line) Q-band EPR spectra of NO (3.1 kPa) introduced in Na-A zeolite at 110 K. The simulation of the NO(II) spectrum was performed using Lorentzian line shape with anisotropic line width of 70, 19, and 40 G for the *x*, *y*, and *z* components, respectively. The other parameters used are given in Table 1. (B) X-band spectrum (dotted line) calculated using the parameters determined from the Q-band simulation compared with the experimental one (solid line) that was recorded for 0.1 kPa NO introduced in Na-A zeolite at 110 K.

as shown in Figure 4. The experimental spectra were well reproduced for both Q-band (Figure 4(A)) and X-band (Figure 4(B)). The best fit EPR parameters employed in the simulation were $g_{xx} = 1.9790$, $g_{yy} = 1.9890$, $g_{zz} = 1.9085$ and $A_{xx}(^{14}N) = A_{zz}(^{14}N) = 0$ G, $A_{yy}(^{14}N) = 30$ G. The averaged g value of NO-(II) is $g_{iso} = 1.9588$ at 110 K; the value is close to that of NO-(I), $g_{iso} = 1.9612$, at 5 K. With regard to the principal values, g_{yy} remained almost unchanged, whereas g_{xx} decreased by 0.0229 and g_{zz} increased by the same amount with respect to the corresponding principal values of NO(I). On the other hand, essentially the same $\boldsymbol{A}(^{14}N)$ values were employed for the simulation of both NO monoradicals. It should be noted that the parameters for NO(II) are close to those reported earlier[7] for the 77 K X-band spectrum of NO adsorbed on Na-A (Table 1).

When the pressure of NO introduced in the zeolite was increased, the signals became broader and stronger, as shown in Figure 2. The features initially unassigned in the spectra were simulated for the S = 1 biradical by adjusting the $\boldsymbol{g}$ tensor and the D and E parameters of the zero field splitting (ZFS) tensor. The best simulation of the EPR spectrum recorded at 5 K is illustrated in Figure 5. The EPR parameters used are shown in Table 1. It was found that in the simulation of the Q-band, the parameter E cannot be neglected in order to obtain the best agreement with the experimental spectrum. The ZFS is of the dipolar electron−electron interaction type, as will be concluded further in the text. The nonvanishing E parameter indicates a deviation from the point-dipole approximation of the ZFS for the biradical. However, the E parameter (28 G) was small in comparison to the D parameter (331 G) and, in contrast to the Q-band simulation, it was not necessary to include in the simulation of the X-band spectrum.[7,8]

Superposition of the calculated spectra of the NO(I) monoradical and the NO biradical with the weighted ratio of 1:1 is shown as the dotted line in Figure 5(b). The experimental and simulated spectra are in satisfactory agreement.

Discussion

NO Monoradical. The existence of two different types of NO monoradicals, NO(I) and NO(II), was indicated by the very particular temperature dependence of the present Q-band spectra. Considering the energy level diagram of NO interacting with

TABLE 1: *g* Tensors, Hyperfine Coupling (*hfc*) Tensors (^{14}N), and Zero-Field Splitting (ZFS) for NO Adsorbed on Sodium Ion-Exchanged Zeolites

		NO monoradical						NO biradical					
zeolite	temp	*g* tensors[a]			*hfc*/G			*g* tensors			ZFS/G[b]		
structure	K	g_{xx}	g_{yy}	g_{zz}	A_{xx}	A_{yy}	A_{zz}	g_{xx}	g_{yy}	g_{zz}	$\|D\|$	$\|E\|$	ref
A-type	5	2.0019[c]	1.9961[c]	1.8856[c]	0[c]	33[c]	0[c]	2.0042	1.9770	1.9120	331	28	this study[e]
	110	1.9790[d]	1.9890[d]	1.9085[d]	0[d]	30[d]	0[d]						this study[e]
	77	1.980	1.987	1.905	~0	30	~0	1.976	1.976	1.912	288	0	[7][f]
Y-type	77	1.989	1.989	1.86									[2][f]
	77	1.986	1.978	1.83	~0	29	~0						[4][f]
mordenite	77	1.990	1.990	1.859									[3][f]
ZSM-5	10	1.980	1.980	1.840	0	33	0						[5][f]
	78	1.980	1.980	1.840	0	33	0						[5][f]

[a] The *z* direction is parallel to the N−O bond. [b] $D_{xx} = D - 3E$; $D_{yy} = D + 3E$; $D_{zz} = -2D$; the *z* direction is parallel to the intermolecular direction of the NO biradical. [c] NO(I) (details in text). [d] NO(II) (details in text). [e] Q-band measurement. [f] X-band measurement.

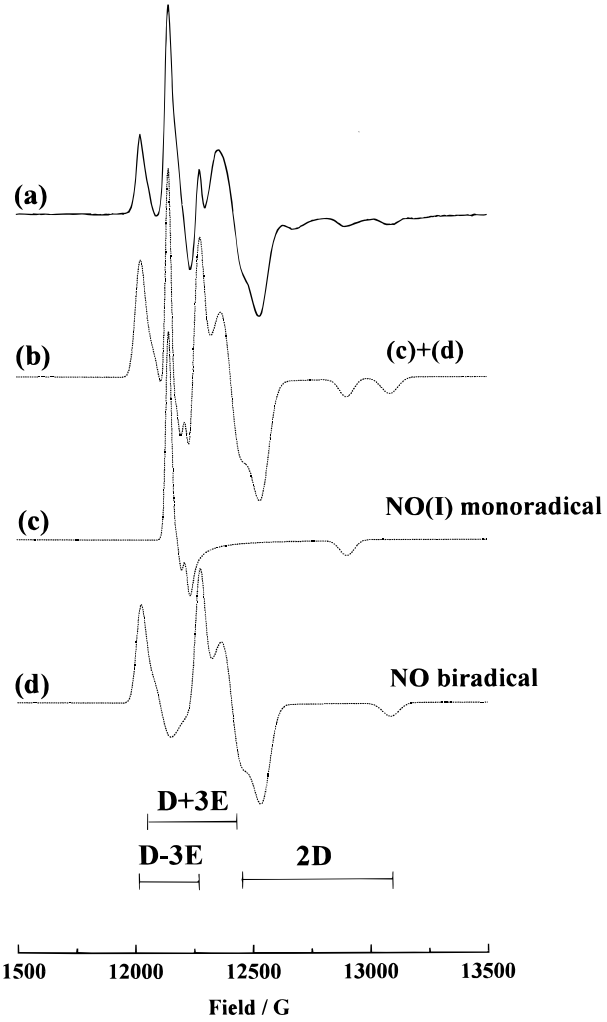

Figure 5. Experimental (solid line) and simulated (dotted line) Q-band EPR spectra of NO (13.2 kPa) introduced in Na-A zeolite at 5 K. The theoretical spectra (c) for NO(I) and (d) for the NO biradical were calculated using Lorentzian line shape with anisotropic line width of 40, 75, and 60 G for the *x*, *y*, and *z* components, respectively. The other parameters used are given in Table 1. The dashed line indicates the simulation of monoradical using the same parameters as in Figure 3 and Lorentzian broadening of 25 G for *x* and *y* components and of 60 G for *z* component. Trace (b) is a superposition of (c) and (d) with the weighted ratio 1:1.

the electrostatic field of the zeolite, an approximate relation between the energy separation and the experimental values of the $\boldsymbol{g}_{zz}$ tensor can be given by[6]

$$\boldsymbol{g}_{zz} = g_e - 2(\lambda/\delta) \quad (1)$$

SCHEME 1

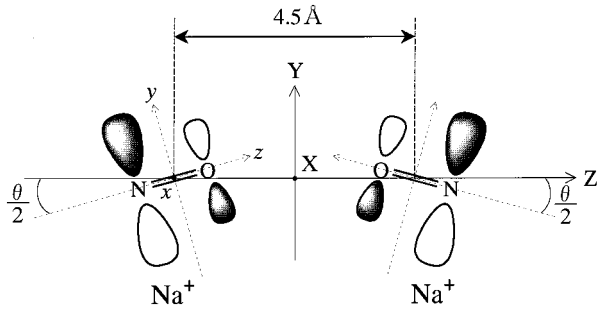

where λ is the spin−orbit coupling constant of NO molecule and δ is the energy separation between the π^*_x and π^*_y orbitals of NO that were split by the interaction with the surface. The *x*, *y*, and *z* directions can be assigned to the molecular coordinate system of NO monomer as shown in Scheme 1. The g_{zz} component is more sensitive to the local environment of zeolites compared with the g_{xx} and g_{yy} components, reflecting the degree of π^* orbital separation in accordance with eq 1. NO(I) possesses a nonaxial $\boldsymbol{g}$ tensor, suggesting a bent structure of Na^+-N-O due to the electrostatic field associated with the zeolitic sodium ions. An alternative possibility is that NO(I) is formed on the aluminum sites of the zeolite framework, more specifically on trigonal aluminum at the oxygen-deficient sites or interstitial aluminum (hydro)oxy cations.[6] However, this possibility can probably be ruled out here because no hyperfine structure from aluminum nuclei ($I = 5/2$) was observed even at 5 K. Here we repeat that NO(II) has *g* and $A(^{14}N)$ parameters close to those reported for the X-band spectrum of NO adsorbed on Na-A at 77 K by Kasai and Bishop.[6] They have also suggested a similar bent structure of NO at a Na^+ adsorption site.

The spectral change between NO(I) and NO(II) was thermally reversible and the total radical concentration remained unchanged in the temperature range studied, as mentioned above. Furthermore, the average *g* value of NO(II) was essentially the same as that of NO(I). These results suggest that the low-temperature type of NO, NO(I), and the high-temperature type of NO, NO(II) possess a similar electronic structure. The most probable explanation to the spectral change is that the former corresponds to a rigid state form and the latter to a rotational state form of an identical NO monoradical. Comparing the $\boldsymbol{g}$ values of NO(II) with those of NO(I), the resonance positions of g_{xx} and g_{zz} were shifted to the higher and lower field sides, respectively, by the same amount of 0.0229, whereas almost the same g_{yy} value was observed for both NO(I) and NO(II). This observation strongly suggests that the rotational motion of NO(II) is highly anisotropic, in which the preferred axis of

rotation is parallel or nearly parallel to the g_{yy} principal direction. Consistent with this view is that $A_{yy}(^{14}N)$ remained almost unchanged when NO(I) was thermally transformed to NO(II). By the rotation about the *y*-axis, $A_{xx}(^{14}N)$ and A_{zz} (^{14}N) values should also be partially averaged. Both the rigid limit values of $A_{xx}(^{14}N)$ and A_{zz} (^{14}N) were, however, close to zero. This can be the reason the original ^{14}N hyperfine principal values remained unchanged after the transformation.

It was observed that for NO(I) the line-width of the g_{zz} component became broader with increasing temperature from 5 to 30 K and the component became invisible above 40 K. Simultaneously a new g_{zz} band of NO(II) grew up as mentioned above. This can be interpreted in terms of the greater sensitivity of the line width (vs the shift in resonance position) due to motional effects. That is, the phenomenon is analogous to the well-known case in magnetic resonance of diatomic radicals similar to NO, for example, O_2^-, where lines first broaden before they shift.[10,11] In the present experiments, the g_{zz} band of NO-(II) was already visible at 20 K before the corresponding band of NO(I) completely disappeared. This can be rationalized by taking a distribution of the rotational rate into consideration. It is natural to expect that the chemical environment of molecules adsorbed or bonded in a complex system like zeolites is heterogeneous rather than homogeneous.[12]

NO Biradical. It is well established that the ZFS of radical pairs, like the present NO biradical, generally originates from the dipolar interaction between the two unpaired electrons of the radical units. The *D* parameter of ZFS depends on the average distance between two radicals, *R*, according to the relation $D = 3g\beta/(2R^3)$.[13] The values of *R* evaluated from the experimental *D* value (331 G) were in the range 4.5 Å, which is almost the same as that estimated from X-band spectra measured by us[8] and Kasai et al.[6,7]

However, the nonvanishing value of the parameter *E* indicated slight deviation of the ZFS tensor from axial symmetry, which is in disagreement with the point dipole approximation. Since the anisotropy of the ZFS can depend on contributions from the spin−orbit (SO) mechanism, we had to rule out the latter independently. If the triplet parameters were due to pure SO effect, the axes of $\boldsymbol{g}$ and $\boldsymbol{D}$ tensors would coincide, and in addition their components would be related according to the following well-established equations:

$$\boldsymbol{g} = \mathbf{1}g_e + 2\lambda\Lambda \tag{2}$$

$$\boldsymbol{D} = \lambda^2\Lambda \tag{3}$$

The dimensionless tensor Λ is given from second-order perturbation theory by the matrix elements of the orbital angular momentum.[14] Rearranging eqs 2 and 3, we obtain the simple equation

$$\lambda = \frac{2\,D_{zz}}{g_{zz} - g_e} \tag{4}$$

which was finally used together with the relation $D_{ZZ} = -2D/3$ to estimate the value of λ using the parameters shown in Table 1. Using the experimental values of $D = 331$ G and $g_{zz} = 1.9120$, the value of 0.8 cm^{-1} was evaluated. This is in clear disagreement with the literature value of the spin−orbit coupling parameter of free NO, approximately 124 cm^{-1}. We conclude therefore that the NO biradical is of dipole−dipole type.

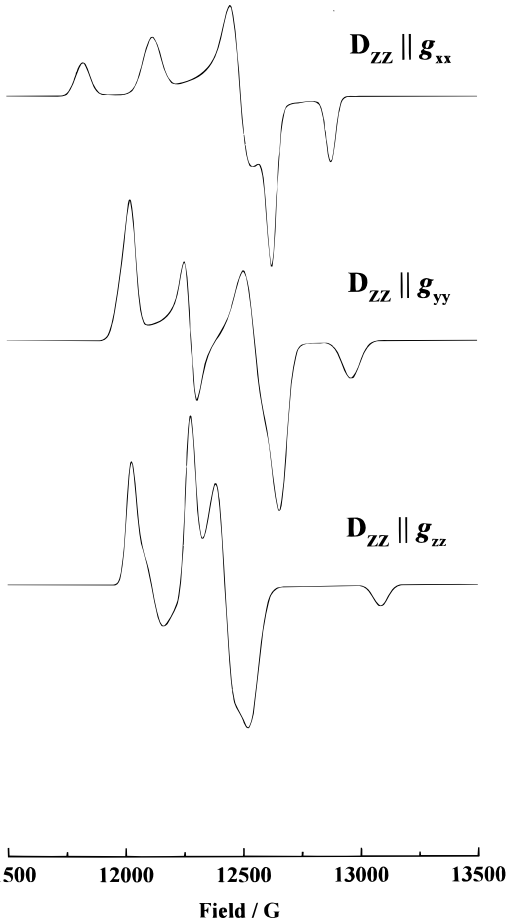

Figure 6. Theoretical EPR line shapes of the biradical calculated for different orientations between the principal axes of g_{ii} ($i = x, y, z$) and D_{zz}. The principal values of g_{ii} and D_{zz} used are given in Table 1. Anisotropic Lorentzian line widths of 40, 75, and 60 G were used for the *x*, *y*, and *z* components, respectively.

The $\boldsymbol{g}$ and $\boldsymbol{D}$ tensors need not always be parallel with each other, and test simulations were performed trying to reproduce in particular the experimental EPR powder line shape of the biradical. Figure 6 shows the theoretical line shapes for the three possible ways that the principal $\boldsymbol{g}$- and $\boldsymbol{D}$-tensor directions can coincide. The biradical line shape was very sensitive with respect to the relative orientations of the $\boldsymbol{g}$ and the $\boldsymbol{D}$ tensors. Best agreement was obtained when g_{zz} and D_{zz} are parallel to each other. Complementary line shape simulations using small deviations from complete coincidence were also carried out using the model in Scheme 1. The system was described by a spin Hamiltonian involving the Zeeman terms of each NO unit and a dipolar coupling between the two unpaired electrons. The principal values of the $\boldsymbol{g}$ tensors of each molecule were the experimental values for the biradical with the principal axes parallel and perpendicular to the NO bond and along the common *x* axis ($g = 2.0042$). The direction of D_{zz} was taken along the line connecting the midpoints of the two N−O bonds. The calculations were made by diagonalization of the spin Hamiltonian matrix with a computer program written for the purpose. The result is depicted in Figure 7. Clearly, the principal axes cannot deviate by more than 30 degrees from each other in this model.

Byberg et al.[15] have investigated the relations of the magnetic parameters of the individual radicals in a radical pair to the parameters of the triplet spectrum. We assume that the expressions given in that work can be used to correlate the NO and

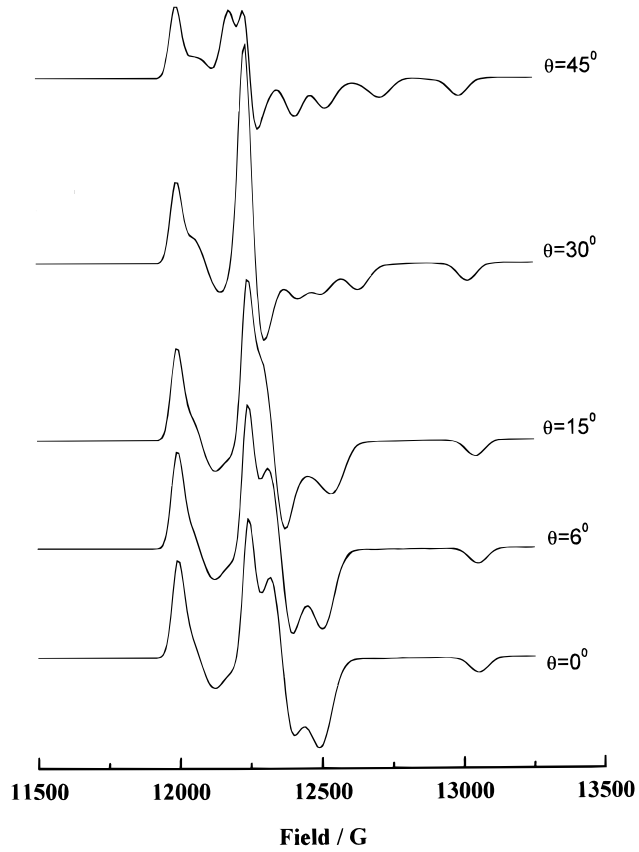

Figure 7. Theoretical EPR line shapes of the biradical calculated for noncollinear principal axes of g_{zz} in the two NO molecules with angle θ (in degree). The angle is defined in Scheme 1. Anisotropic Gaussian line widths of 40, 75, and 60 G for the *x*, *y*, and *z* components were used for the calculations.

NO−NO parameters obtained here. In particular, the expression

$$\boldsymbol{g} = \frac{1}{2}(\boldsymbol{g}_a + \boldsymbol{g}_b) \tag{5}$$

relates the $\boldsymbol{g}$ tensor of a radical pair to the tensors of the two constituent radicals *a* and *b*. In the case when $\boldsymbol{g}_a = \boldsymbol{g}_b$, it follows that $\boldsymbol{g} = \boldsymbol{g}_a$, which was not observed experimentally. One possible explanation is that the interacting NO units are orientated as shown in Scheme 1. With an angle $\theta = 54$ degrees between the NO bonds, we obtain $g_{yy} = 1.9733$ and $g_{zz} = 1.9084$, in fair agreement with the experimental values for the biradical. Obviously, the tilt angle obtained in this model is quite large. However, working with powders and not having independent structural information limits our ability to obtain a detailed structure.

The ^{14}N coupling in the monoradical exhibited appreciable splitting specifically for the *y*-direction, as seen in Table 1. We note also, that both the direction and the magnitude of the hyperfine splitting in the monoradical was unusually stable with respect to temperature, and even remained the same for other types of zeolite. In contrast, the ^{14}N splitting was never observed in the biradical. It was expected that the ^{14}N splitting in the biradical should show half the value of that in the monoradical.[15] Taking the small ^{14}N coupling in the monoradical (ca. 30 G) into account, it may be difficult to resolve the ^{14}N splitting in the biradical in the present study.

Kasai and Gaura[7] have proposed that the biradical formed in A-zeolite has the structure shown in Scheme 1, with closely parallel N−O bond directions. Since the $\boldsymbol{g}$ tensor and $\boldsymbol{D}$ parameter of the biradical determined in the present study are similar to those reported in earlier X-band studies,[7,8] and although a nonzero *E*-parameter had to be added here, it seems plausible that this structure of the biradical is also consistent with the present Q-band study. In the present study, no direct evidence could be obtained for the interaction between biradical and sodium ions. However, on the basis of our previous experimental results[8] the biradical should in addition involve sodium ions located in the eight-member rings. A pictorial overview of the above features is shown in Scheme 1. Further study on the details of the geometrical structure of the biradical and the monoradicals found in Na-A zeolite is currently in progress.

Conclusions

A Q-band EPR study was carried out for Na-A zeolite with adsorbed NO. Well-resolved EPR spectra of NO radicals were observed in a wide temperature range from 5 to 140 K, which allowed us to determine accurate EPR parameters of both NO monoradical and NO−NO biradical adsorbed in the zeolite by the EPR line shape simulation method. Two different types of EPR spectra were observed for the NO monoradical. One is a low-temperature type spectrum which was observed below 30 K. The other is a high-temperature type spectrum observed in the temperature range between 20 and 110 K. Its EPR $\boldsymbol{g}$ and $\boldsymbol{A}(^{14}\mathrm{N})$ parameters were close to the previously reported values[6] for the X-band spectrum of NO adsorbed on Na-A at 77 K. Based on the thermal reversibility of the spectral change and the experimental ESR parameters, the former was attributed to a rigid form and the latter to a rotational form of the same NO monoradical. A likely rotation axis of the NO monoradical was suggested by comparing the EPR parameters for the two forms. Furthermore, the structure of the biradical, first detected in the present Q-band experiments, was discussed based on the $\boldsymbol{g}$ and zero field $\boldsymbol{D}$ tensors. It was concluded that (a) the coupling between the two unpaired electrons must essentially be of dipole−dipole type, with almost coaxial $\boldsymbol{g}$ and $\boldsymbol{D}$ tensors, and (b) that the two NO units in the biradical have $\boldsymbol{g}$ tensors that deviate from that of the monoradical.

Acknowledgment. The present study was partially supported by grants from the Swedish Foundation for International Cooperation in Research and Higher Education (STINT), the Swedish National Technical Reserch Board (TFR), and Saneyoshi Foundation. N.P.B. is indebted to the Swedish Royal Academy of Sciences (KVA) and the Japanese Society for the Promotion of Science (JSPS). We thank the referee for valuable comments regarding the temperature dependence of NO monoradical spectra and the structure of NO biradical.

References and Notes

(1) Iwamoto, M.; Yahiro, H. *Catal. Today* **1994**, *25*, 5.
(2) Lunsford, J. H. *J. Phys. Chem.* **1968**, *72*, 4163.
(3) Gardner, C. L.; Weinberger, M. A. *Can. J. Chem.* **1970**, *48*, 1317.
(4) Kasai, P. H.; Bishop, R. J., Jr. *J. Am. Chem. Soc.* **1972**, *94*, 5560.
(5) Gutsze, A.; Plato, M.; Karge, H.; Witzel, F. *J. Chem. Soc., Faraday Trans.* **1996**, *92*, 2495.
(6) Kasai, P. H.; Bishop, R. J., Jr. *Zeolite Chemistry and Catalysis*; Rabo, J. A., Ed.; ACS Monograph 171; American Chemical Society: Washington, DC, 1976; p 350.
(7) Kasai, P. H.; Gaura, R. M. *J. Phys. Chem.* **1982**, *86*, 4257.
(8) Biglino, D.; Li, H.; Erickson, R.; Lund, A.; Yahiro, H.; Shiotani, M. *Phys. Chem. Chem. Phys.* **1999**, *1*, 2887.
(9) These authors indicated only one type of NO monoradical in ref 7, while we have evidence of at least two different types, as discussed further in the text.

(10) Shiotani, M.; More, G.; Freed, J. *J. Chem. Phys*. **1981**, *74*, 2616.
(11) Tatsumi, K.; Shiotani, M.; Freed, J. *J. Phys. Chem.* **1983**, *87*, 3425.
(12) Li, H.; Yahiro, H.; Shiotani, M.; Lund, A. *J. Phys. Chem. B* **1998**, *102*, 5641.
(13) Gillbro, T.; Lund, A. *J. Chem. Phys.* **1974**, *61*, 1469.
(14) Carrington, A.; MacLachlan A. D. *Introduction to Magnetic Resonance with Applications to Chemistry and Physical Chemistry*; Harper and Row: New York, 1967; p 135.
(15) Byberg, J. R.; Bjerre, N.; Lund, A.; Samskog, P.-O. *J. Chem. Phys.* **1983**, *78*, 5413.